Supporting Information

ITO-Free Large Area PDLC Smart Windows: A Cost-Effective Fabrication Using Spray Coated SnO_2 on Invisible Al Mesh

Indrajit Mondal [a], S. Kiruthika [a,b,⊥], Mukhesh K. Ganesha [a,⊥], Marlin Baral[a], Ankush Kumar[c], S. Vimala [a], P. Lakshmi Madhuri [a], Geetha G. Nair[a,*], S. Krishna Prasad[a,*], Ashutosh K. Singh[a], and Giridhar U. Kulkarni[a,c*]

[a]*Centre for Nano and Soft Matter Sciences, Bangalore-562162, India.*
[b]*Department of Physics, School of Electrical & Electronics Engineering (SEEE), SASTRA Deemed University, Thanjavur 613 401, Tamil Nadu, India.*
[c]*Chemistry & Physics of Materials Unit, Jawaharlal Nehru Centre for Advanced Scientific Research, Bangalore-560064, India.*

* Corresponding authors
E-mail addresses: Dr. S. Krishna Prasad (skpras@gmail.com), Prof. Giridhar U. Kulkarni (gukulk@gmail.com, kulkarni@jncasr.ac.in), Dr. Geetha G. Nair (geeraj88@gmail.com)

Component	Electrode (ITO: 2 no.)	NOA65	E7 liquid crystal	Spacer
Price	40-50 $	10-15 $	10-15$	1-2 $

Supporting Information Table S1. Component wise price distribution for a 1 ft^2 ITO/PDLC/ITO device.

Sl. No.	**System**	**PDLC**			**Gel**		
		τ_{ON} (ms)	τ_{OFF} (ms)	V_{th} (V)	τ_{ON} (ms)	τ_{OFF} (ms)	V_{th} (V)
1	ITO/ITO	44	80	1.42	16	37	0.8
2	ITO/Au_SnO_2 mesh	49	270	1.23	20	72	1.03
3	Au_SnO_2/Au_SnO_2 mesh	62	170	1.28	20	144	1.02

τ_{ON} = Response time; τ_{OFF} = Recovery time; V_{th} = Threshold voltage

Supporting Information Table S2. Hybrid mesh-based LC device comparison with the ITO-based standard device.

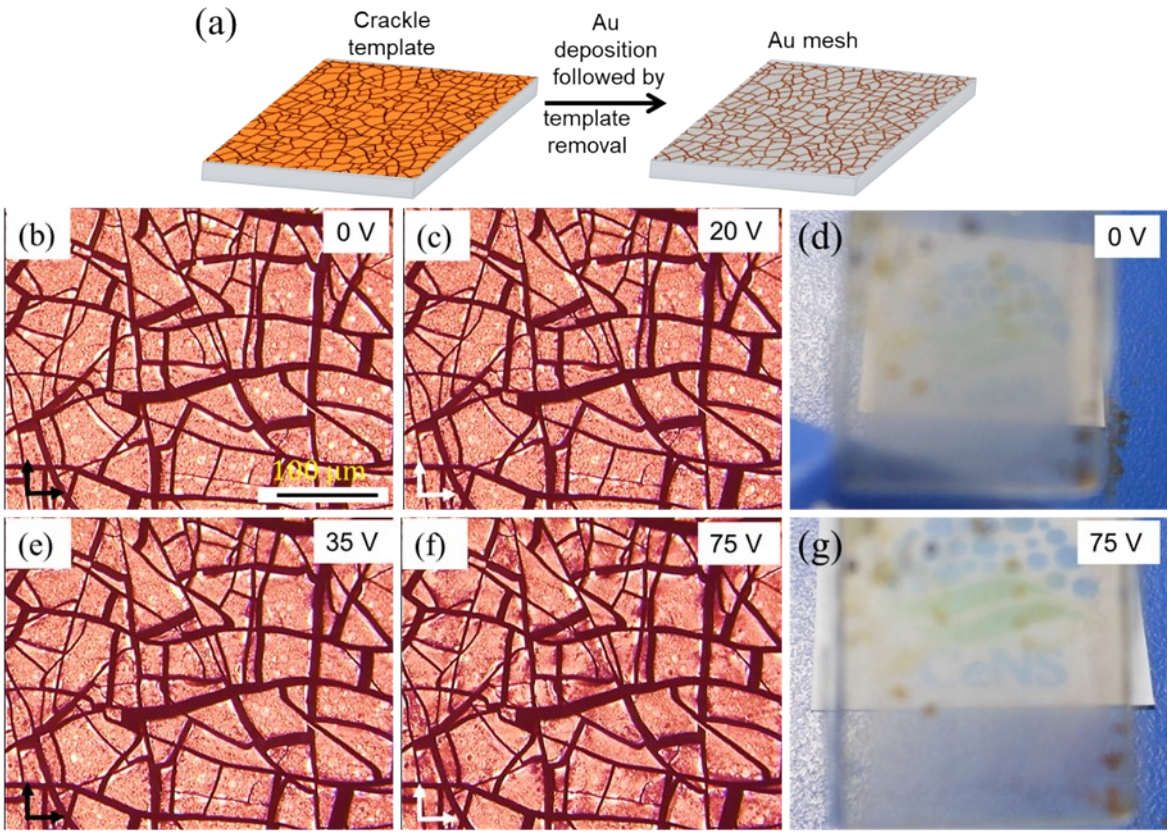

Figure S1. (a) Schematic representation of metal mesh fabrication by crackle lithography: coating crackle precursor and drying to form crackle template, and metal evaporation followed by template removal. Polarizing Optical microscopy images of a Au mesh/PDLC/Au mesh device at applied voltage of (b) 0 V, (c) 20 V, (e) 35 V and (f) 75 V (transmission mode). Digital photograph of the device at (d) OFF (0 V) and (g) ON (75 V) state.

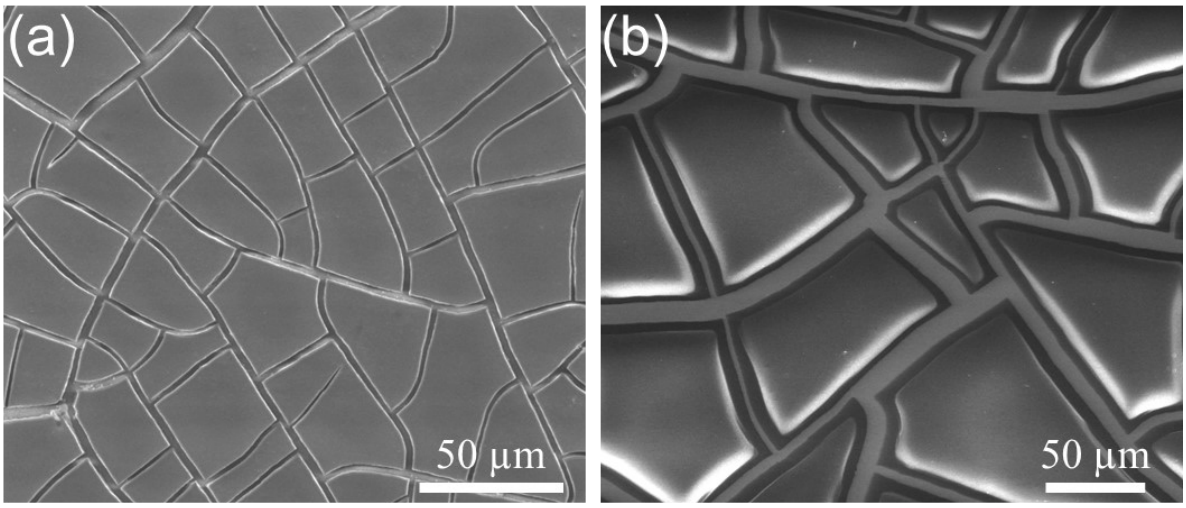

Figure S2. (a) FESEM image of the crackle template and (b) Au mesh. A charging effect is observed in the Au mesh image due to the presence of non-conducting regions between the mesh polygon.

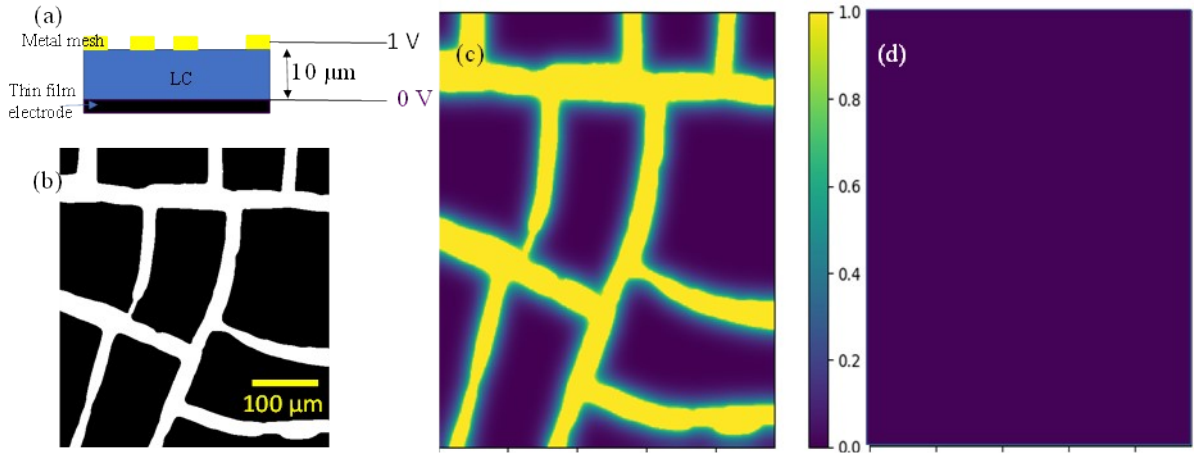

Figure S3. (a) 3-dimensional potential distribution modeling in the LC film of 10 µm thickness sandwiched between the metal network and a conducting thin film counter electrode. (b) Binary image of a metal network. Potential distribution at the (c) surface of the metal network and (d) surface of the thin film electrode. The potential distribution modeling is performed by a self-written finite element method approach coded in python.

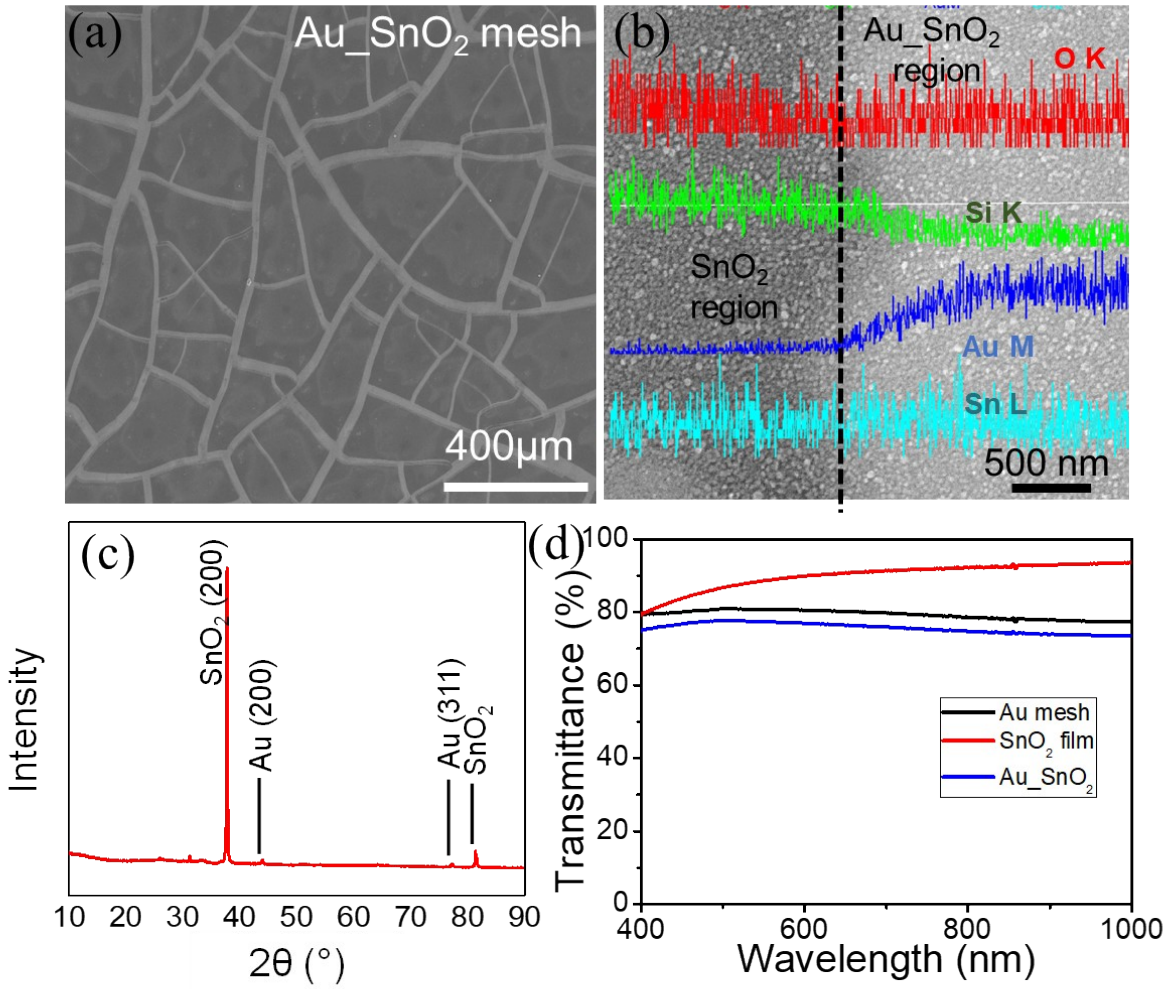

Figure S4. (a) low and (b) high magnification FESEM images of the hybrid TCE; the line mapping indicates the uniform coating of SnO_2 film across the bare glass and Au mesh coated region. (c) XRD plot indicating the presence of peaks corresponding to both Au and SnO_2. (d) Transmission plot for Au mesh, pristine SnO_2 film and the hybrid electrode.

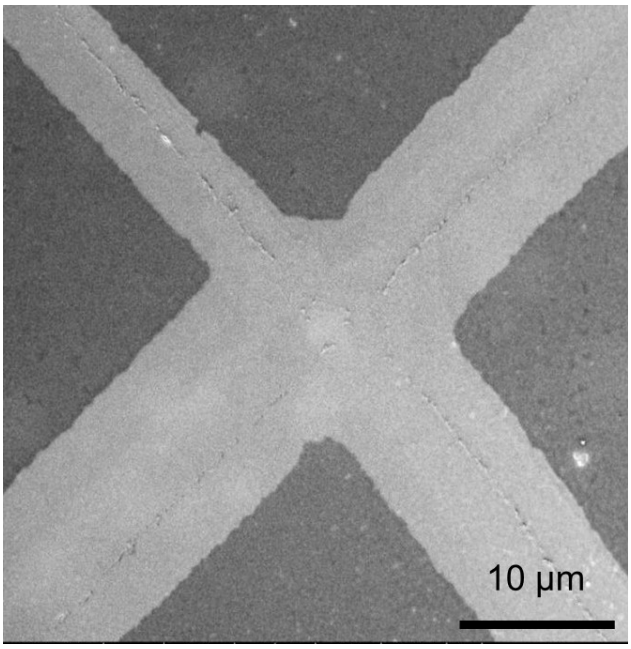

Figure S5. FESEM image showing a seamless junction of the Au mesh.

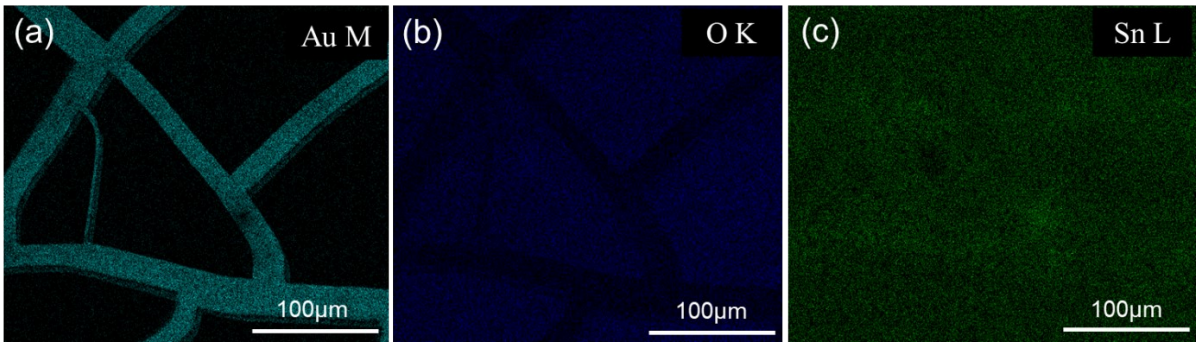

Figure S6. EDS mapping of (a) Au, (b) O and (c) Sn confirming the uniform coating of SnO_2 on Au mesh.

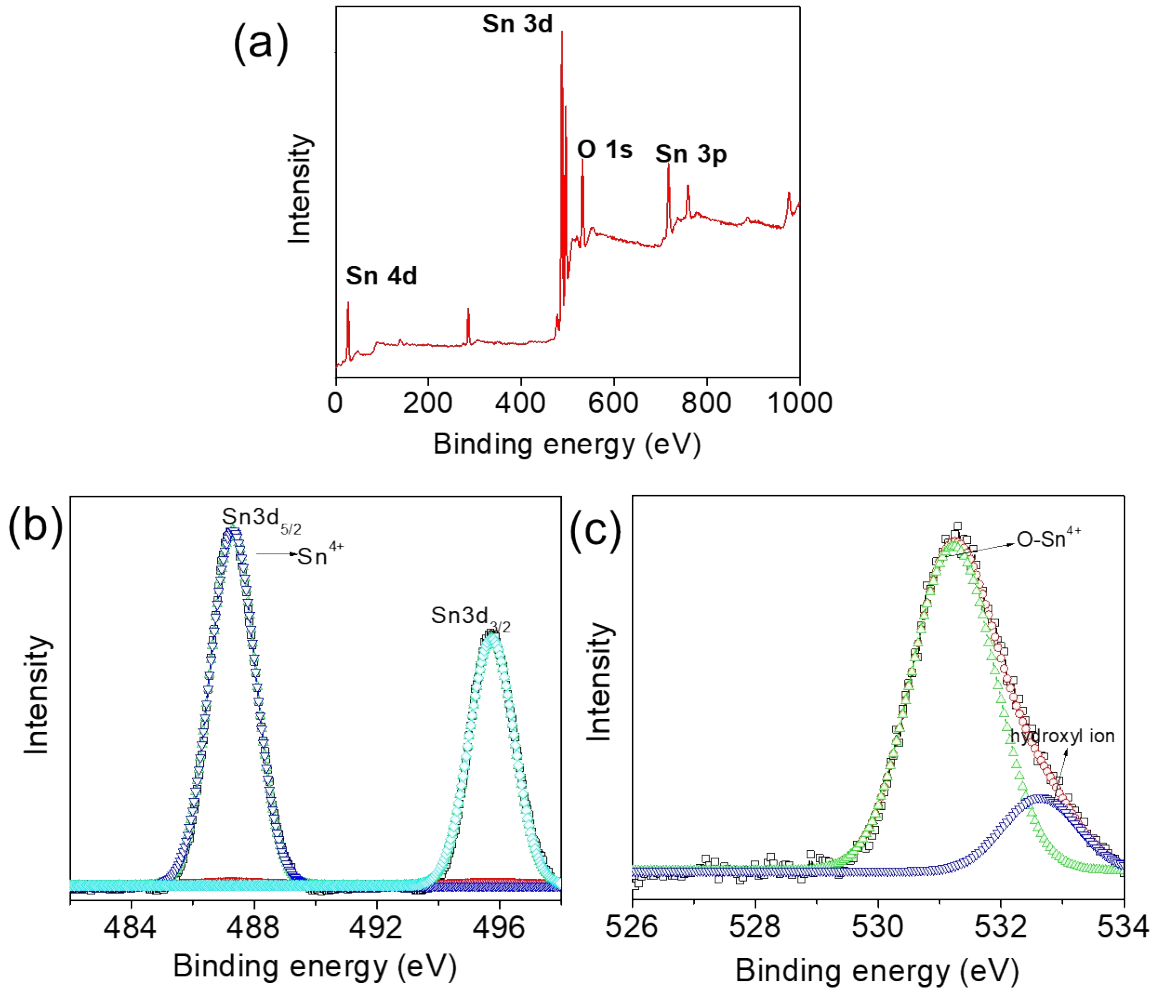

Figure S7. (a) X-ray photoelectron spectroscopic (XPS) measurement of SnO_2 film. High-resolution (b) Sn_{3d} and (c) O_{1s} XPS spectra of SnO_2

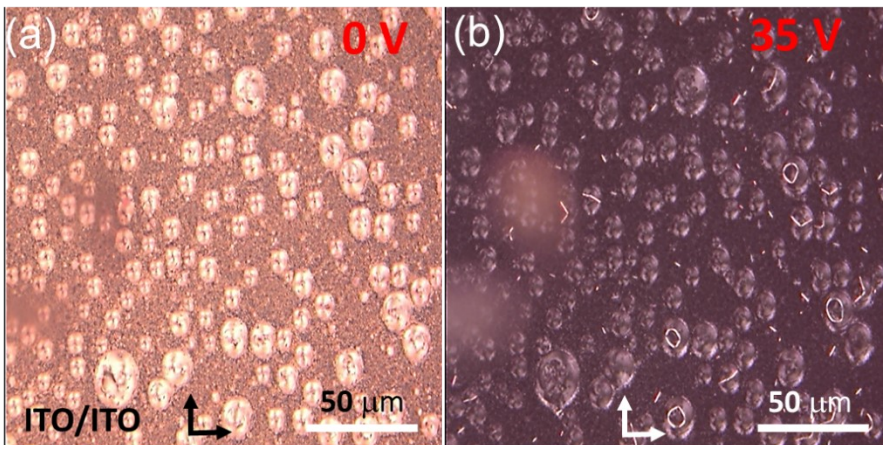

Figure S8. Polarizing optical microscopic images in (a) OFF and (b) ON state of a PDLC device fabricated using ITO electrodes. The clear contrast difference indicates a proper device switching. The arrow marks indicate the direction of the crossed polarisers.

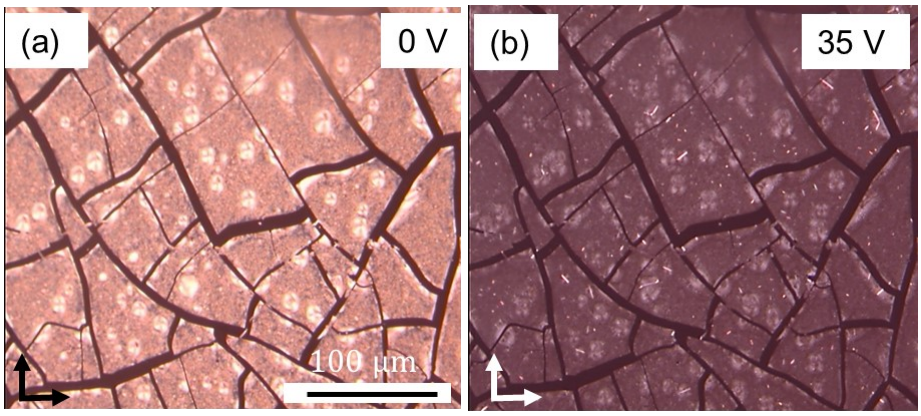

Figure S9. Polarizing optical microscopic images of ITO/PDLC/Au_SnO_2 device in its (a) OFF and (b) ON state.

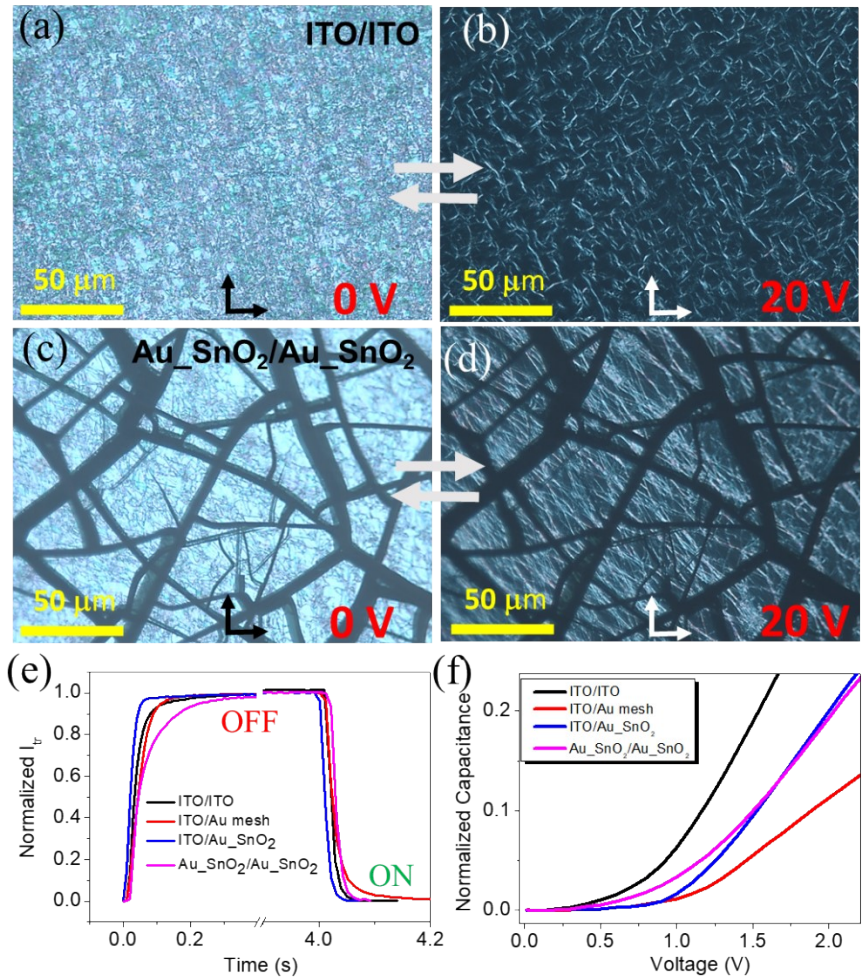

Figure S10. Polarizing optical microscopic images of Gel devices fabricated using (a)-(b) ITO/ITO and (c)-(d) Au_SnO_2 /Au_SnO_2 electrodes in their OFF and ON states. (e) Electro-optic response and recovery plots. (f) Freedericksz transformation behavior: normalized capacitance versus applied voltage profiles for various combinations of electrodes.

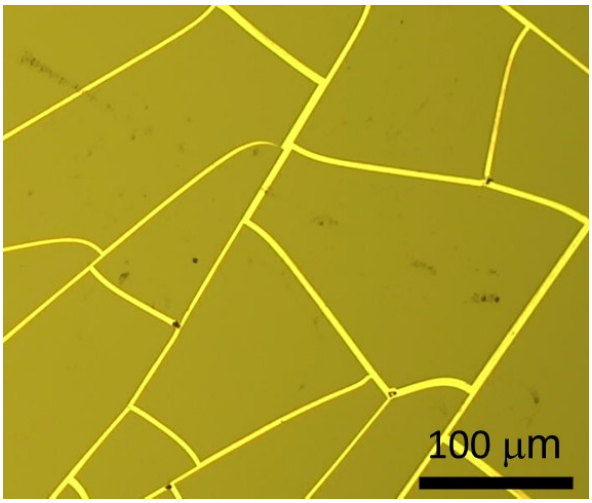

Figure S11. Optical microscopy image of an interconnected Al mesh electrode.

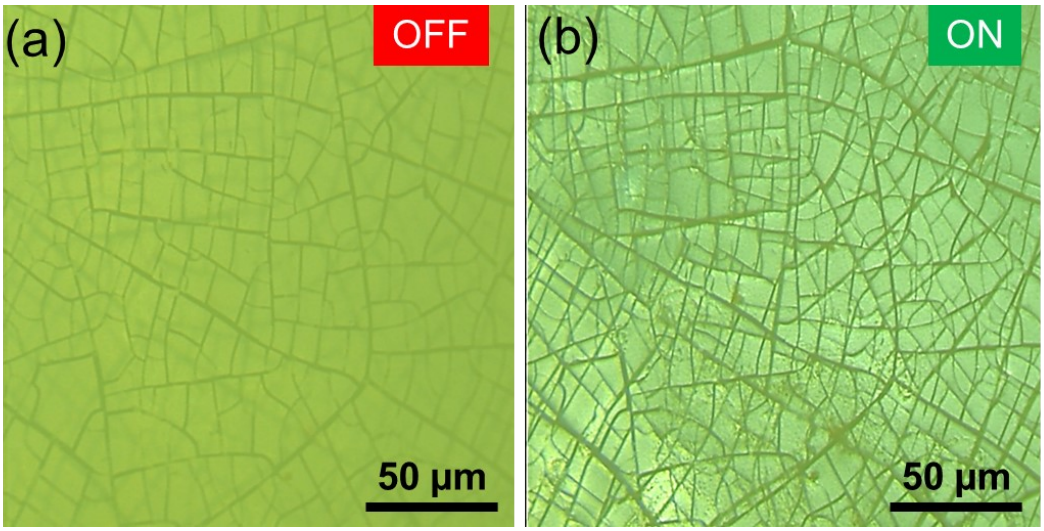

Figure S12. Optical microscopic images of Al_ SnO_2/PDLC/Al_SnO_2 device in its (a) OFF and (b) ON state. The bottom electrode mesh is also visible in the ON-state, representing the PDLC layer becoming transparent upon applying the electric field.

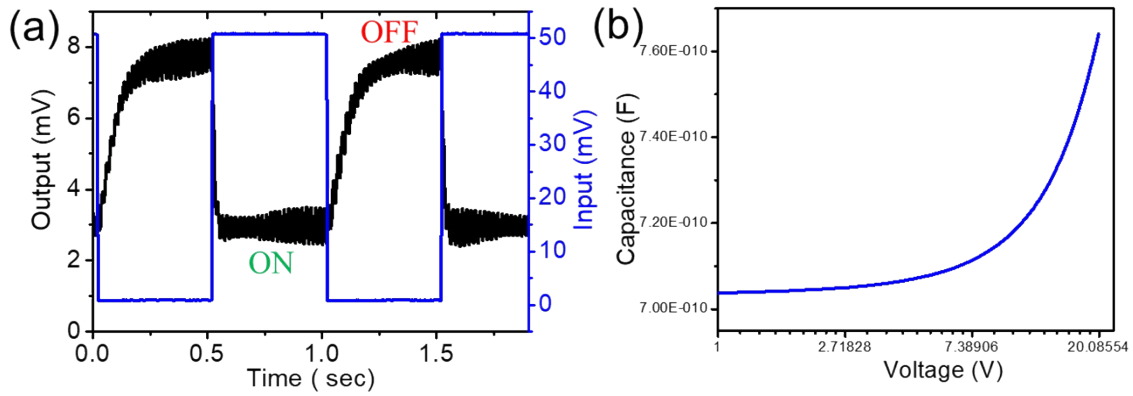

Figure S13. (a) Electro-optic response recovery of Al_SnO_2/PDLC/Al_SnO_2 device and (b) Freedericksz transformation behavior.

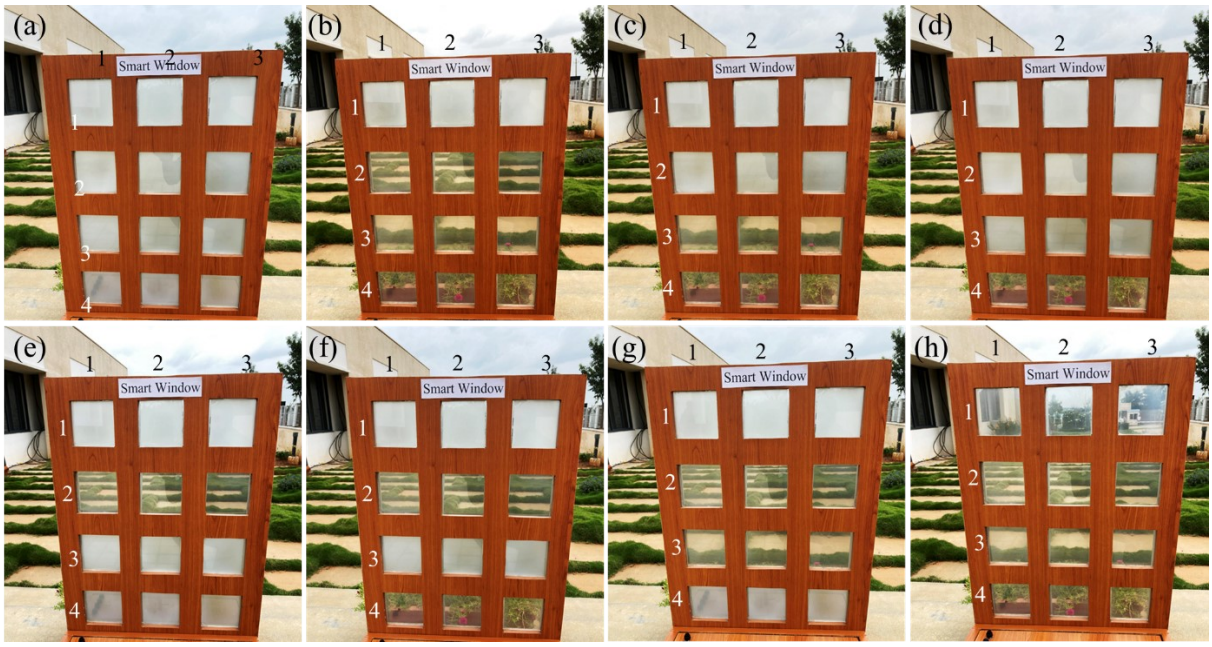

Figure S14. Photographs of a smart window-cum-display device (daylight view) in its fully opaque (a), partially transparent (b)-(g), and fully transparent states (h).

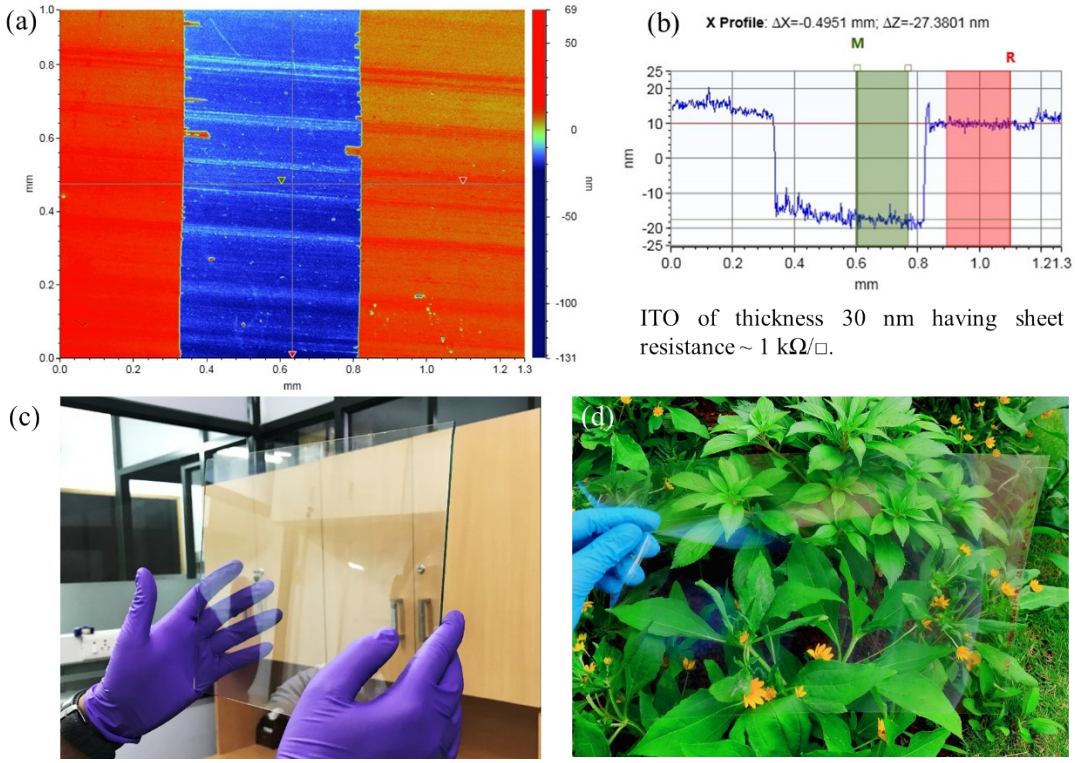

ITO of thickness 30 nm having sheet resistance ~ 1 kΩ/□.

Figure S15. (a) Optical profilometry image of a ITO thin film and (b) the corresponding thickness profile. Large-area Al_ITO hybrid TCE on (c) glass and (d) flexible PET substrate.

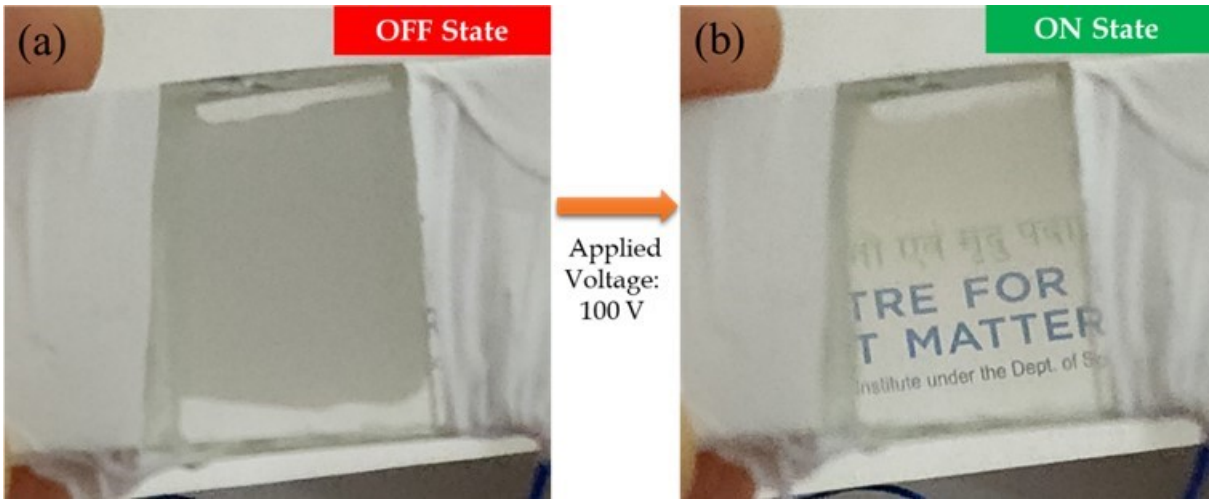

Figure S16. PDLC device made of Al_ITO as the transparent electrodes in its (a) OFF and (b) ON state.

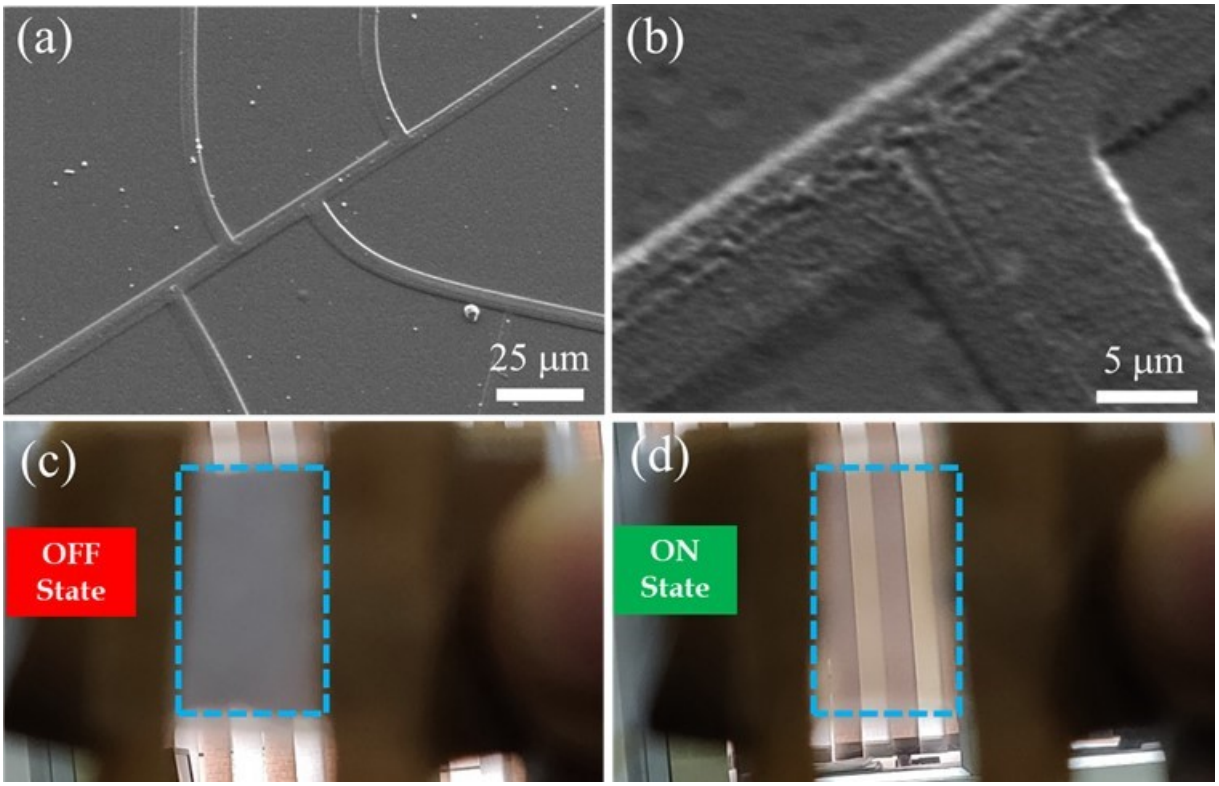

Figure S17. (a) Low and (b) high mag. FESEM images of PEDOT:PSS coated Al mesh electrode. A PDLC device comprised of the Al_PEDOT:PSS hybrid electrodes in its (c) OFF and (d) ON states.